

[View the Full Text HTML](#)



P-Derived Organic Cations as Structure-Directing Agents: Synthesis of a High-Silica Zeolite (ITQ-27) with a Two-Dimensional 12-Ring Channel System

Douglas L. Dorset,^{*,†} Gordon J. Kennedy,[†] Karl G. Strohmaier,[†]
Maria J. Diaz-Cabañas,[‡] Fernando Rey,[‡] and Avelino Corma^{*,‡}

Contribution from Corporate Strategic Research, ExxonMobil Research and Engineering Company, Annandale, New Jersey 08801, and Instituto de Tecnología Química, University Politécnica de Valencia, Valencia, Spain

Received February 20, 2006; E-mail: d.l.dorset@exxonmobil.com; acorma@itq.upv.es

Abstract: Recently, efforts have been made to synthesize large-pore, multidimensional zeolite frameworks as a basis for new catalysts to improve various hydrocarbon conversions. A new aluminosilicate zeolite, ITQ-27, has been prepared using the phosphorus-containing structure-directing agent, dimethyldiphenylphosphonium. Its crystal structure was determined in its calcined form by direct methods (FOCUS) on synchrotron powder diffraction data ($\lambda = 0.8702 \text{ \AA}$) after the unit cell and space group were determined from tilt electron diffraction experiments on individual microcrystals. The material crystallizes in space group *Fmmm*, where $a = 27.7508(5) \text{ \AA}$, $b = 25.2969(7) \text{ \AA}$, and $c = 13.7923(4) \text{ \AA}$. The final model, refined by Rietveld methods, comprises seven unique T-sites forming a framework with straight 12-MR channels that are connected by 14-MR openings between them. (Corresponding 12-ring pore dimension is $6.94 \text{ \AA} \times 6.20 \text{ \AA}$.) Since access from one 14-MR opening to the next is through the 12-MR channel, the structure is best described as a two-dimensional, 12-MR framework.

Introduction

The synthesis of microporous materials aims to construct a porous space that would support dimensionally constrained catalytic conversions. Various organic structure-directing agents (SDAs) have been tested with the aim of controlling the pore shape as the inverse of the three-dimensional molecular template topology. Although a direct analogy between template and resultant channel space cannot always be demonstrated, there is ample evidence that the SDA does have an influence on defining the channel geometry.¹ While SDAs are traditionally tetraalkylammonium cations, other types of SDAs such as macrocyclic ethers² and organometallic cations³ have also been employed. We have recently begun to investigate the use of tetraalkylphosphonium cations as structure-directing agents. These compounds do not give the Hoffmann degradation reaction, being more thermally stable than tetraalkylammonium cations and allowing more severe crystallization conditions.

In the search for intersecting large-pore zeolites to process large hydrocarbon molecules, two major approaches have been used for their exploratory synthesis. One has been to employ fluoride ions instead of hydroxide, and the other has been to

insert unusual heteroatoms into the T-site framework,⁴ such as Ge. The former approach has the advantage that fluoride partially functions as a templating agent⁵ to induce the formation of highly siliceous compositions.^{6,7} The latter is beneficial because resultant smaller Ge–O–Ge and Ge–O–Si bond angles stabilize the formation of the double four-ring (D4R) structure building unit (SBU) often associated with these materials.⁸ Computational studies reveal that germanium contents of 2–3 atoms per D4R are most energetically favorable.⁹

This paper describes the synthesis and crystal structure determination of ITQ-27, a new two-dimensional large-pore aluminosilicate synthesized via the fluoride procedure with a tetraalkylphosphonium SDA.

Experimental Section

The aluminosilicate was synthesized using diphenyldimethylphosphonium hydroxide (Scheme 1) as a SDA in a fluoride medium. The diphenyldimethylphosphonium template was obtained by methylation of diphenylphosphine with methyl iodide in chloroform in the presence of K_2CO_3 . It was then converted to the corresponding hydroxide with

[†] Corporate Strategic Research.

[‡] Instituto de Tecnología Química.

(1) Szostak, R. S. *Molecular Sieves*, 2nd ed.; Blackie Academic & Professional: London, 1998.

(2) Delprato, F.; Delmotte, L.; Guth, J. L.; Huve, L. *Zeolites* **1990**, *10*, 546.

(3) Lobo, R. F.; Tsapatsis, M.; Freyhardt, C. C.; Khodabandeh, S.; Wagner, P.; Chen, C. Y.; Balkus, Jr., K. J.; Zones, S.I.; Davis, M. E. *J. Am. Chem. Soc.* **1997**, *119*, 8474.

(4) Corma, A.; Diaz-Cabañas, M. J.; Martinez-Triguero, J.; Rey, F.; Rius, J. *Nature* **2002**, *418*, 514.

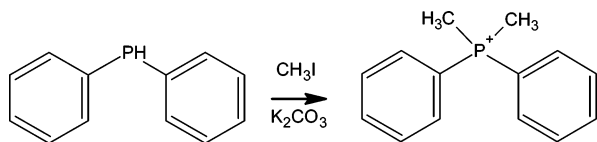
(5) Guth, J. L.; Kessler, H.; Higel, J. M.; Lamblin, J. M.; Patarin, J.; Seive, A.; Chezeau, J. M.; Wey, R. *ACS Symp. Ser.* **1989**, *398*, 176.

(6) Cambor, M. A.; Villaescusa, L. A.; Diaz-Cabañas, M. J. *Top. Catal.* **1999**, *9*, 59.

(7) Corma, A.; Rey, F.; Rius, J.; Sabater, M. J.; Valencia, S. *Nature* **2004**, *431*, 287.

(8) Castaneda, R.; Corma, A.; Fornes, V.; Rey, F.; Rius, J. *J. Am. Chem. Soc.* **2003**, *125*, 7820.

(9) Sastre, G.; Vidal-Moya, J. A.; Blasco, T.; Ruis, J.; Jorda, J. L.; Navarro, M. T.; Rey, F.; Corma, A. *Angew. Chem., Int. Ed.* **2002**, *41*, 4722.

Scheme 1. Synthesis of Diphenyldimethylphosphonium

an anionic exchange resin in batch overnight. The synthesis was carried out under hydrothermal conditions in Teflon-lined stainless steel autoclaves and continuous stirring from a gel of composition:

SiO₂: 0.014 Al₂O₃: 0.50 Me₂Ph₂POH: 0.50 HF: 4.2 H₂O

In this synthesis, 9.73 g of tetraethyl orthosilicate (TEOS) and 0.28 g of aluminum isopropoxide were hydrolyzed in 86.01 g of diphenyldimethylphosphonium hydroxide (Me₂Ph₂POH) solution with a concentration of 0.27 mol/1000 g of solution. The mixture was then stirred at room temperature until the Si and Al precursors were completely hydrolyzed and the water and alcohol evaporated to the final gel concentration. Finally, 0.97 g of a HF solution (48 wt %) was added, and the mixture was homogenized by stirring and was autoclaved at 150 °C under tumbling for 59 days. The solid recovered by filtration, washed with distilled water, and dried at 373 K is pure ITQ-27. Elemental analysis gave: 38.2 Si, 1.24 Al, 2.49 P, 13.52 C, 1.25 H, and 0.50 F (wt %), indicating that the SDA molecule is intact within the zeolite channels. The pure crystallized zeolite was calcined in air for 3 hours at 580 °C to remove the organic template and fluorine. Elemental analysis of the calcined sample after calcination (2.0 wt % P) showed that the phosphorus was not completely removed.

Conventional X-ray diffraction measurements on a calcined/hydrated sample were measured on a laboratory instrument with Cu K α radiation with Bragg–Brentano geometry. A calcined/dehydrated sample was prepared for Debye–Scherrer X-ray diffraction measurement by outgassing the calcined/hydrated ITQ-27 sample in a sealed quartz capillary at 300 °C under vacuum (<0.1 Torr). The synchrotron powder diffraction measurement of this sample was made at the ExxonMobil beam line X10B ($\lambda = 0.87020$ Å) at the Brookhaven National Laboratory. The room-temperature pattern was measured from 3 to 50° 2 θ with a 0.005° step size. In addition to single-crystal electron diffraction evaluations (see below) patterns were also indexed with the Jade software.¹⁰ The crystal structure was solved using the direct methods software package FOCUS.¹¹ Rietveld refinements of the structural models were made with software program GSAS,¹² with the crystallographic data given in Table 1. Silicate models used for Rietveld refinement were first geometrically refined by DLS¹³ to optimize bonding parameters.

Absorption measurements were performed on samples calcined in air at 580 °C for 3 hours.

Transmission electron diffraction measurements were initially carried out at 200 kV with a JEOL JEM-2010 electron microscope, an instrument that did not permit tilting of the specimen. Later, $\pm 45^\circ$ goniometric tilts of individual microcrystals around reciprocal lattice rows were permitted with the use of a 300 kV FEL/Philips CM-30 instrument. The zeolite sample was first crushed to a fine powder in a mortar and pestle and then suspended in acetone in an ultrasonic bath. Drops of the fine particle suspension were then dried on carbon-film-covered 300-mesh copper electron microscope grids. Selected area electron diffraction patterns were recorded on Kodak SO-163 electron

Table 1. Crystallographic Refinement Data for ITQ-27

molecular formula	Al ₅ Si ₁₄₇ O ₃₀₄
formula weight	9127.3
<i>a</i> (Å)	27.7508(5)
<i>b</i> (Å)	25.2969(7)
<i>c</i> (Å)	13.7923(4)
<i>V</i> (Å ³)	9682.3(3)
<i>Z</i>	1
space group	<i>Fm</i> <i>mmm</i> (no. 69)
calculated density	1.565 g/cm ³
<i>T</i> (°C)	25
λ Å	0.8702
<i>N</i> _{obs}	9400
<i>R</i> ² _F	11.8%
χ^2	3.77
<i>R</i> _{wp} ^a	11.5%
expected <i>R</i> _{wp} ^b	5.9%

^a $R_{wp} = \{\sum w(I_o - I_c)^2 / \sum w I_o^2\}^{1/2}$ where *I*_o = observed intensity of each point and *I*_c = calculated intensity of each point. ^b Expected $R_{wp} = R_{wp} / \{\chi^2\}^{1/2}$.

microscope film, developed in Kodak HRP developer. Reciprocal spacings in diffraction patterns were calibrated against a gold powder standard.

All of the solid-state NMR measurements were made at room temperature. The ²⁷Al, ²⁹Si MAS, and ²⁹Si CPMAS NMR spectra were recorded on a Varian InfinityPlus-500 spectrometer operating at 11.7 T (¹H 499.2 MHz) corresponding to 130 and 99 MHz. Larmor frequencies for ²⁷Al and ²⁹Si, respectively. ²⁹Si MAS (Bloch decay) and CPMAS NMR were recorded using a 7.5 mm Varian probe at spinning speeds of 4 and 3.5 kHz, respectively. ²⁹Si MAS (Bloch decay) data were recorded with ¹H decoupling during data acquisition, 4 μ s $\pi/2$ pulses, a 60 s pulse delay, and 720 scans were collected. ²⁹Si CP/MAS data were recorded with ¹H decoupling during data acquisition, 4 μ s $\pi/2$ pulses, 3.5 ms contact time, a 3 s pulse delay, and 4000 scans were collected. ²⁷Al MAS (Bloch decay) NMR spectra were recorded using a 4 mm Varian probe at spinning speeds of 10 kHz with ¹H dipolar decoupling during data acquisition, 1.2 μ s $\pi/2$ pulses, a 0.3 s pulse delay, and 1600 scans were collected. The ¹³C and ³¹P MAS NMR spectra were recorded on a Varian InfinityPlus-400 spectrometer operating at 9.4 T (¹H 399.4 MHz) corresponding to Larmor frequencies of 100.4 and 161.7 MHz, respectively. ¹³C MAS (Bloch decay) NMR spectra were recorded using a 4 mm Varian probe at spinning speeds of 10 kHz with ¹H dipolar decoupling during data acquisition, 1.8 μ s $\pi/2$ pulses, a 60 s pulse delay, and 2400 scans were collected. ³¹P MAS (Bloch decay) NMR spectra were recorded using a 7.5 mm Varian probe at spinning speeds of 5 kHz with ¹H dipolar decoupling during data acquisition, 4 μ s $\pi/2$ pulses, a 300 s pulse delay, and 8 scans were collected. The ²⁷Al and ³¹P chemical shifts are referenced with respect to external solutions of Al(H₂O)₆³⁺ ($\delta_{Al} = 0.0$ ppm) and 85% H₃PO₄ ($\delta_P = 0.0$ ppm), respectively. The ¹³C and ²⁹Si chemical shifts are referenced with respect to external solutions of tetramethylsilane with $\delta_C = 0.0$ ppm and $\delta_{Si} = 0.0$ ppm. The ¹⁹F MAS NMR spectra were recorded at an ¹⁹F frequency of 469.667 MHz on a Varian InfinityPlus (11.7 T) NMR spectrometer using a 3.2 mm MAS probe, 18 kHz spinning speed, 4 μ s pulses, 240 scans, and a 20 s pulse delay.

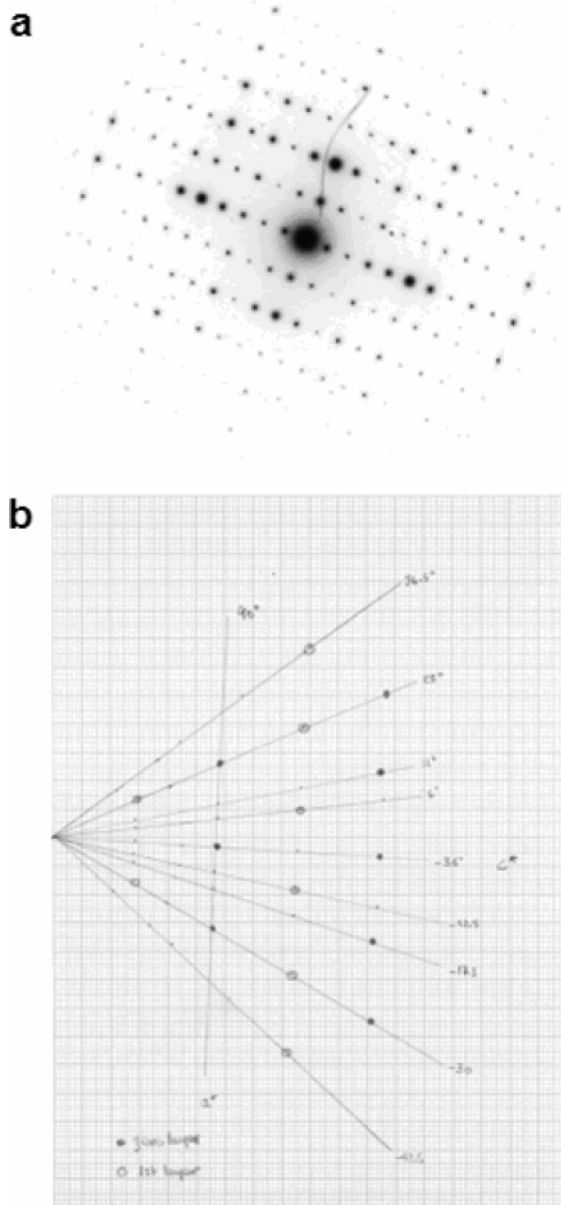
Results

Pure samples of ITQ-27 can be recovered from aluminosilicate synthesis after relatively long crystallization times (59 days). Subsequent attempts to prepare ITQ-27 with seeds from previous synthesis only shortened the crystallization time by one week. The porosity of the calcined ITQ-27 sample was measured by adsorbing nitrogen and argon, and the results obtained are given in Table 2. The micropore volume of 0.21 cm³/g and pore diameter of 6.7 Å indicate that the material is most likely a two-dimensional, possibly three-dimensional, large-pore zeolite.

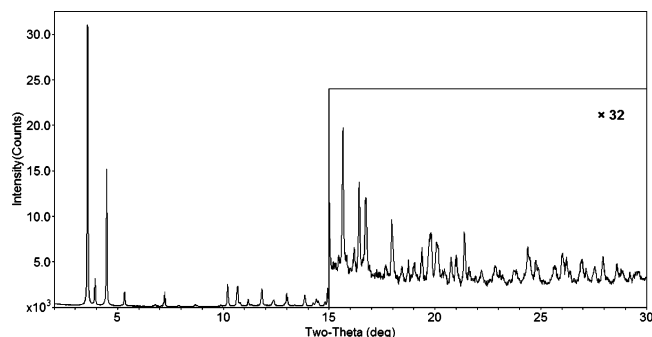
- (10) Jade 6: XRD Analysis Software, ver. 6.5.10; Materials Data, Inc.: Livermore, CA, 2003.
 (11) Grosse-Kunstleve, R. W.; McCusker, L. B.; Baerlocher, Ch. *J. Appl. Crystallogr.* **1999**, *32*, 536.
 (12) Larsson A. C.; von Dreele, R. B. GSAS: General Structure Analysis System; Los Alamos Laboratory: Los Alamos, NM, 1994.
 (13) Baerlocher, Ch.; Hepp, A.; Meier, W. M. *Distance Least Squares Refinement Program, DLS-76*; ETH: Zürich, 1977.

Table 2. Porosity of ITQ-27 from N₂ and Ar Absorption Measurements

BET surface area	450 m ² /g
micropore area	434 m ² /g
micropore, volume	0.21 cm ³ /g
pore diameter	6.7 Å

**Figure 1.** Electron diffraction of ITQ-27. (a) Pattern (0kl) from untilted crystal. (b) Representative tilt series around a reciprocal axis to map out reciprocal lattice net.

While electron diffraction measurements of untilted zeolite microcrystals can be helpful for determining the unit cell and space group, the results from ITQ-27 were rather confusing, pointing to a number (at least five) of possible zonal projections, some with *c*-centered and some with primitive symmetry. These various patterns could not be compromised unequivocally with attempts to index a laboratory powder X-ray pattern. A rectangular zonal projection could be found at near zero tilt (Figure 1) that measured approximately 12.82 Å × 7.00 Å. Previous ambiguities were resolved by goniometric sampling

**Figure 2.** Synchrotron powder pattern from calcined ITQ-27.

of the three-dimensional reciprocal lattice. Tilts around each reciprocal axis row produced two representations of projected rectangular nets yielding cell constants for an orthorhombic cell: $a = 27.72$ Å, $b = 25.64$ Å, and $c = 14.00$ Å. Observed systematic absences indicate for the *hkl* net that $h+1 = 2n$, $h+k = 2n$ reflections are observed, pointing to an *F*-centered space group: *F222*, *Fmm2*, or *Fmmm*. Observed primitive reflection rules are: $0kl$: $k = 2n$, $l = 2n$; $hk0$: $h = 2n$, $k = 2n$; $h0l$: $h = 2n$, $l = 2n$, also consistent with these space group choices.¹⁴ Earlier observations of *c*-centered patterns did not correspond to zonal projections. Rather, these represented accidental tilted views of the individual microcrystals. This unit cell/space group option had been a choice in the earlier attempt to index laboratory powder data and was unequivocally confirmed when the synchrotron powder pattern data (Figure 2) were analyzed.

After Le Bail extraction¹⁵ of powder structure factor magnitudes via GSAS,¹² assuming equal partitioning of overlapping peaks, the structure analysis was attempted with both laboratory and synchrotron data via FOCUS.¹¹ Using either synchrotron or laboratory data, a single framework model was found with seven unique T-sites. After providing linkage oxygen atoms, DLS refinements¹³ of the model yielded $R = 0.0048$ before the seventh cycle parameters derived from the least-squares refinement of the unit cell. If the cell axes were allowed to refine during DLS, $R = 0.0078$ before the ninth cycle, the cell volume increases by only 4.7% with a largest axial increase of 3.3%. The framework model is depicted in Figure 3. Inspection of the calculated diffraction patterns of the proposed model showed a close match to the experimental pattern. Analysis of the difference Fourier electron density maps could find no evidence of the extraframework phosphorus species, probably due to its low occupancy and/or indicating a disordered state.

Starting with the DLS coordinates, two Rietveld refinements were carried out, again with GSAS,¹² one imposing interatomic distance restraints suggested in earlier work:¹⁶ $d_{\text{Si-O}} = 1.61$ -(1), $d_{\text{O-O}} = 2.61$ (15) Å, and the other with interatomic distance restraints: $d_{\text{Si-O}} = 1.61$ (3), $d_{\text{O-O}} = 2.65$ (6) Å. The latter refinement model (Table 3), resulting in unit cell constants $a = 27.7508$ (5) Å, $b = 25.2969$ (7) Å, and $c = 13.7923$ (4) Å, gives the most reasonable bonding results (Supporting Information) with Si–O bonds between 1.55 and 1.67 Å and with O–Si–O bond angles near the tetrahedral value ($109.3 \pm 3.2^\circ$). The bond distances are within the range found in an earlier

(14) Hahn, Th., Ed. *Space Group Symmetry*; International Tables for Crystallography, Volume A; Kluwer: Dordrecht, 1995.

(15) Le Bail, A.; Duroy, H.; Fourquet, J. L. *Mater. Res. Bull.* **1988**, *23*, 447.

(16) Olson, D. H.; Khosrovani, N.; Peters, A. W.; Toby, B. N. *J. Phys. Chem. B* **2004**, *104*, 4844.

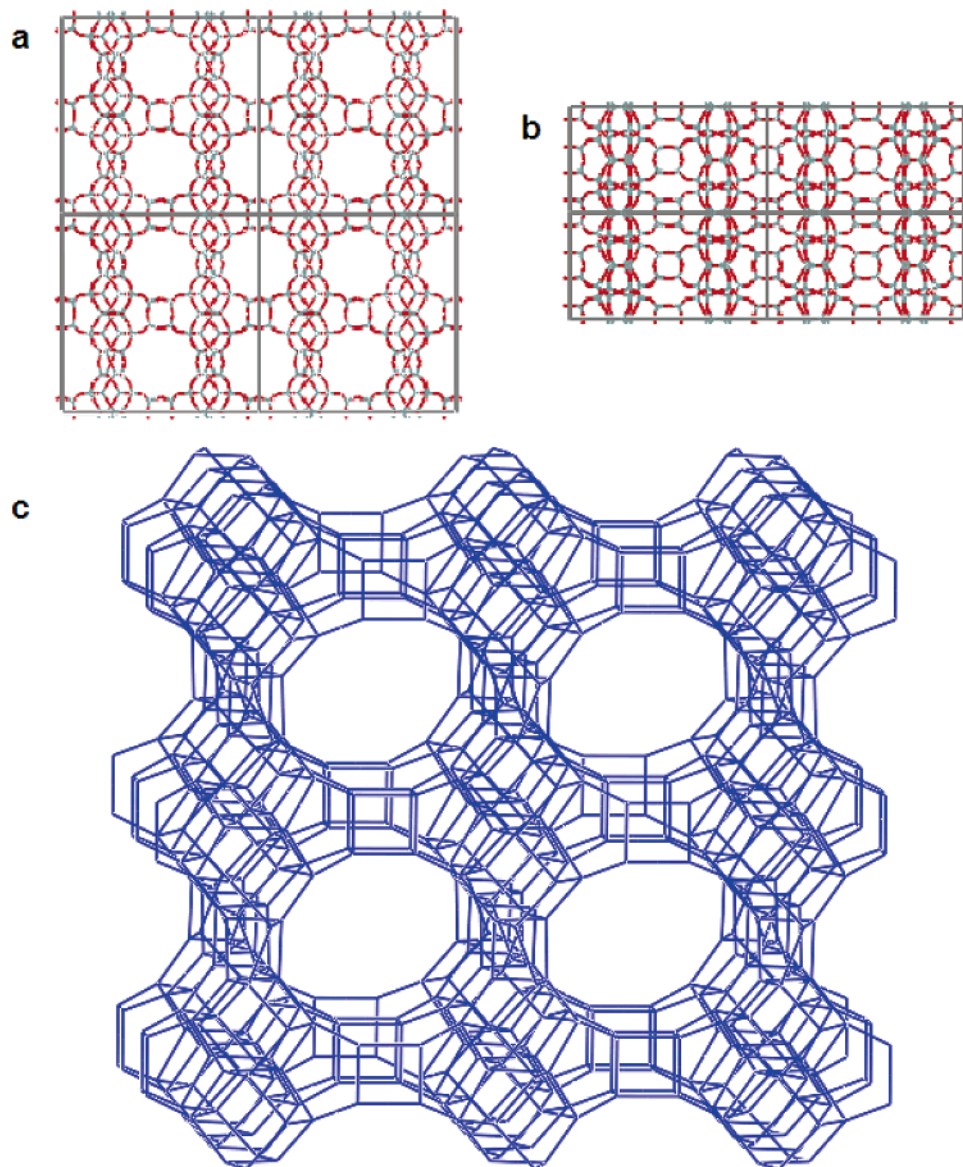


Figure 3. Structural framework of ITQ-27. (a) [001]; (b) [010]; (c) [001], framework T-atoms only.

refinement of ZSM-5.¹⁷ Aside from four values at or very close to 180° , designating a statistical average, the T–O–T angles range from 135.1 to 170.7° when a value of 145° is expected. (T–O–T bond angle values near 180° are thought to represent an average over an infinite set of displaced O-positions with varying occupancies.¹⁸) Moreover, the peak profile parameters are nearest to expected value ranges with a small negative value for GV. The final figures of merit for the fit to the experimental pattern (Figure 4) are $R_{wp} = 0.1150$, $R(F^2) = 0.1178$, $\chi^2 = 3.77$. Coordination sequence¹⁹ and vertex symbols²⁰ are given in the Supporting Information.

Finally the silicate crystal density is calculated to be 1.565 gm/cm^3 and the T-site framework density is $15.7 \text{ T}/1000 \text{ \AA}^3$. This is close to the average of $15.5 \text{ T}/1000 \text{ \AA}^3$ for the 17 other known D4R-containing zeolite frameworks.²¹

Discussion

From its crystal structure, ITQ-27 is seen to be a two-dimensional framework comprising straight 12-MR channels in one direction ([001]). Along a second direction ([010]) are tortuous channels containing 14-MR openings connecting the 12-MR channels, but they are arranged in such a manner that a molecule must transverse one-half of a unit cell along the 12-MR channel to arrive at the next 14-MR opening. Therefore, the structure is best described as a two-dimensional 12-MR framework. Along the [001] axis, the continuous channels measure $6.9 \text{ \AA} \times 6.2 \text{ \AA}$, similar to the values found for other 12-ring pores, although somewhat elliptical in shape. Along the [010] axis, the opening for the tortuous channel mouth measures $8.5 \text{ \AA} \times 7.2 \text{ \AA}$, similar to a value found for the 14-ring pore of AET.²² These results are consistent with the absorption measurements in Table 2 that indicate the presence of a multidimensional system with large pore channels.

The ^{27}Al MAS spectrum of ITQ-27, shown in Figure 5, consists of a single resonance at $\delta_{\text{Al}} = 54.5 \text{ ppm}$, corresponding

(17) Olson, D. H.; Kokotailo, G. T.; Lawton S. L.; Meier, W. M. *J. Phys. Chem.* **1981**, *85*, 2238.

(18) Lawton, L.; Rohrbaugh, W. J. *Science* **1990**, *247*, 1319.

(19) Meier W. M.; Moeck, H. J. *J. Solid State Chem.* **1979**, *27*, 349.

(20) O'Keeffe M.; Hyde, S. T. *Zeolites* **1997**, *19*, 370.

(21) Baerlocher, Ch.; McCusker, L. B. Database of Zeolite Structures: <http://www.iza-structure.org/databases/>.

(22) Dessau, R. M.; Schlenker, J. L.; Higgins, J. B. *Zeolites* **1990**, *10*, 522.

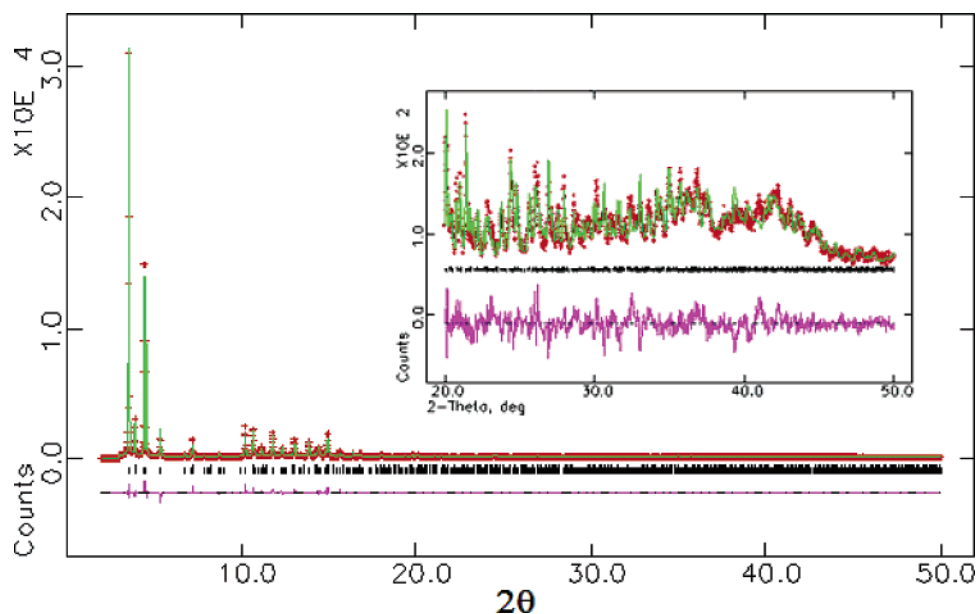


Figure 4. Fit of model in Figure 3 to synchrotron data profile.

Table 3. Atomic Coordinates of ITQ-27 after Rietveld Refinement^a

atom	x/a	y/b	z/c
Si1	0.1478(2)	0.0995(2)	0.1968(4)
Si2	0.3033(2)	0	0.2101(4)
Si3	0.0544(2)	0.0656(2)	0.1128(4)
Si4	0.2800(3)	0.1959(2)	0
Si5	0.3068(2)	0.1934(2)	0.2129(4)
Si6	0.2050(2)	0.1011(3)	0
Si7	0.2704(4)	0	0
O8	0.0908(2)	0.0951(4)	0.1829(7)
O9	0.1725(3)	0.1027(5)	0.0948(3)
O10	0.1534(3)	0.1539(3)	0.2514(8)
O11	0.1693(3)	0.0519(2)	0.2551(7)
O12	0.25	0	0.25
O13	0.3040(3)	0	0.0946(3)
O14	0.0575(7)	0	0.1204(1)
O15	0.0634(6)	0.0831(6)	0
O16	0	0.0841(7)	0.1429(1)
O17	0.3126(3)	0.1930(4)	0.9034(3)
O18	0.2428(5)	0.1483(3)	0
O19	0.25	0.25	0
O20	0.25	0.1846(7)	0.25
O21	0.3264(5)	0.25	0.25
O22	0.2362(4)	0.0502(2)	0

^a $U_{Si} = 0.015 \text{ \AA}^2$; $U_O = 0.032 \text{ \AA}^2$.

to tetrahedrally coordinated Al. No O_h Al is detected. Comparison of the spectral intensity with a ZSM-5 standard indicated that there is 1.03 wt % T_d Al in this sample, close to that found by elemental analysis in the as synthesized form (1.24 wt %).

The ^{29}Si MAS spectrum of ITQ-27, shown in Figure 6, consists of several resonances due to the combined effects of first-coordination sphere environments (that is the number of nearest-neighbor Al and Si) and crystallographic site inequivalencies on the observed chemical shifts. The multiple overlapping resonances with peak maximum at $\delta_{Si} = -110$ and -117 ppm are both due to crystallographically inequivalent $\text{Si}(\text{OSi})_4$ environments. The peak centered at $\delta_{Si} = -104$ ppm appears to be due to overlap of $\text{Si}(\text{OSi})_4$ and $\text{Si}(\text{OAl})(\text{OSi})_3$ environments. Similarly, the shoulders at $\delta_{Si} = -102$ and -96 ppm are due to $\text{Si}(\text{OAl})(\text{OSi})_3$ and $\text{Si}(\text{OAl})_2(\text{OSi})_2$ environments, respectively.

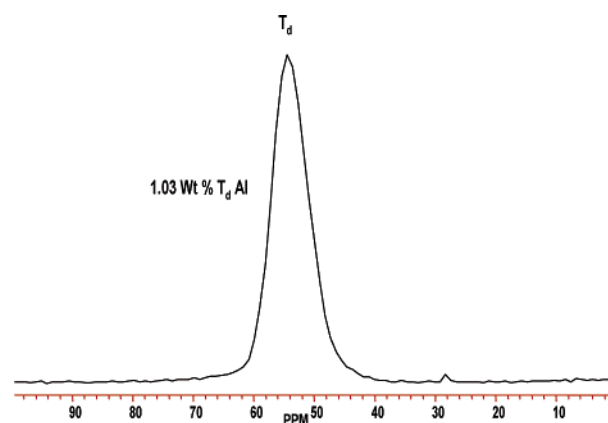


Figure 5. ^{27}Al MAS NMR spectrum of ITQ-27.

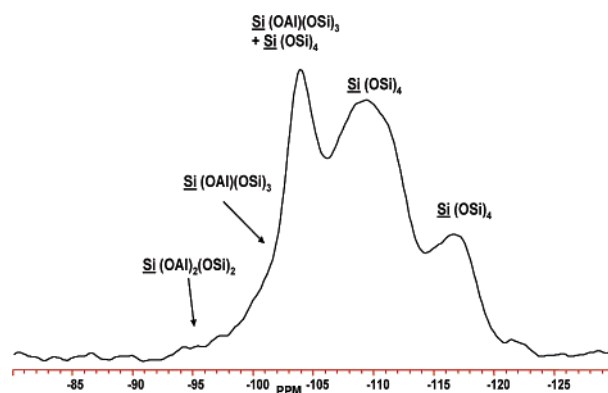


Figure 6. ^{29}Si MAS NMR spectrum of ITQ-27.

The ^{13}C MAS and ^{31}P MAS NMR spectra of as-synthesized ITQ-27, shown in Figures 7 and 8, are consistent with intact SDA. The three major peaks in the ^{13}C spectrum at $\delta_C = 8.3$, 119.1, and 129.9 ppm in the relative ratio of 1:1:5 are due to the methyl, nonprotonated aromatic, and protonated aromatic carbons, respectively, of the SDA. The ^{31}P MAS NMR spectrum consists of a single peak centered at $\delta_P = 19.5$ ppm. This shift is consistent with the intact SDA, and the line width suggests a distribution of environments.

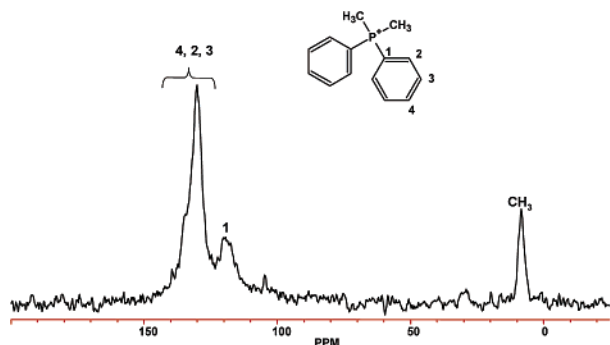


Figure 7. ^{13}C MAS NMR spectrum of ITQ-27.

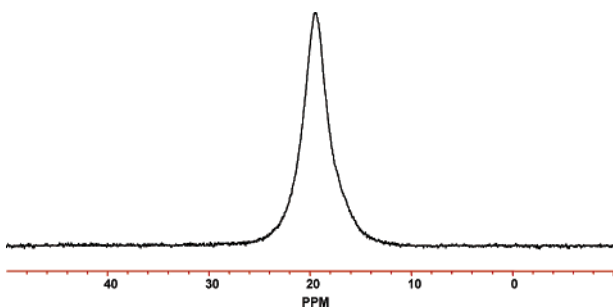


Figure 8. ^{31}P MAS NMR spectrum of ITQ-27.

Although there are several aluminosilicate zeolites (LTA, UZM-5, ITQ-7, and ITQ-12) containing D4R secondary building units, most of the recent new D4R-containing structures have been synthesized with germanium. This new material is notable since it does not require germanium. It has been found that in the absence of germanium, fluoride can also induce the formation of small, four-member ring-containing cavities, including the D4R, in pure silica zeolites.²³ To determine the nature of the fluorine in the structure ^{19}F MAS NMR spectra were recorded on as-synthesized and calcined ITQ-27. The as-synthesized sample shows resonances at -31.6 , -120.6 , and -136.4 ppm. The -31.6 ppm peak is in a spectral region similar to that previously reported for F^- in D4Rs,²³ and the other two

(23) Villaescusa, L. A.; Cambor, M. A. *Recent Res. Dev. Chem.* **2003**, *1*, 93.

peaks are likely impurities such as an Al oxyfluoride species²⁴ and K_2SiF_6 ,²⁵ respectively. All three resonances disappear upon calcination, indicating the complete removal of fluoride from the structure.

Note: It has been brought to our attention²⁶ that the ITQ-27 is structurally related to the NES framework.²⁷ By a simple σ expansion along the z direction of the idealized $Fmmm$ NES framework,²¹ D4Rs are formed and the ITQ-27 framework is generated.

Conclusion

The crystal structure of the new aluminosilicate zeolite, ITQ-27, has been solved from powder X-ray diffraction data using the program FOCUS. The material crystallizes in space group $Fmmm$, where $a = 27.7508(5)$ Å, $b = 25.2969(7)$ Å, and $c = 13.7923(4)$ Å. The final model, refined by Rietveld methods, comprises seven unique T-sites, forming a framework with a straight 12-MR channels with 14-MR openings connecting the 12-MR channels. Since access from one 14-MR opening to the next is through the 12-MR channel, the structure is best described as a two-dimensional, 12-MR framework. Both absorption measurements and NMR spectroscopy are in agreement with the structural model, which contains D4R secondary building units. Finally, the synthesis of ITQ-27 using diphenyldimethylphosphonium as the SDA substantiates the use of phosphonium cations as SDAs in zeolite syntheses.

Acknowledgment. The NMR spectra were recorded with the assistance of C. E. Chase. Helpful discussions with K. D. Schmitt and M. Afeworki are also gratefully acknowledged.

Supporting Information Available: Table of interatomic distances and angles, tables of vertex symbols and coordination sequences, and an X-ray crystallographic (CIF) file of atomic coordinates. This material is available free of charge via the Internet at <http://pubs.acs.org>.

JA061206O

(24) Chupas, P. J.; Corbin, D. R.; Rao, V. N. M.; Hanson, J. C.; Grey, C. P. *J. Phys. Chem. B* **2003**, *107*, 8327.

(25) Kiczanski, T. J.; Stebbins, J. F. *J. Non-Cryst. Solids* **2002**, *306*, 160.

(26) van Koningsveld, H. personal communication, June 2006.

(27) Shannon, M. D.; Casci, J. L.; Cox, P. A.; Andrews, S. J. *Nature* **1991**, *353*, 417.